Formation of Nitrogen-Vacancy Centers in Homoepitaxial Diamond Thin Films Grown via Microwave Plasma-Assisted Chemical Vapor Deposition

Hideyuki Watanabe, Hitoshi Umezawa, Toyofumi Ishikawa, Kazuki Kaneko, Shinichi Shikata, Junko Ishi-Hayase, and Kohei M. Itoh

***Abstract*—A model for controlling the two-dimensional distribution of negatively charged nitrogen-vacancy (NV^-) fluorescent centers near the surface of a diamond crystal is presented, using only a microwave plasma-assisted chemical vapor deposition (CVD) method. In this approach, a CVD diamond layer is homoepitaxialy grown via microwave plasma-assisted CVD using an isotopically enriched methane ($^{12}CH_4$), hydrogen (H_2), and nitrogen (N_2) gas mixture on patterned diamond (0 0 1). When the surface is imaged by means of confocal microscope photoluminescence mapping, fine grooves are observed to have been generated artificially on the diamond surface. NV^- centers are found to be distributed selectively into these grooves. These results demonstrate an effective means for the formation of NV^- centers of selectable size and density via microwave plasma-assisted CVD, with potential application in the production of diamond quantum sensors.**

***Index Terms*—Diamond, doping, nitrogen-vacancy centers, groove structure, homoepitaxial, microwave plasma-assisted chemical vapor deposition.**

Manuscript received July 27, 2015; revised January 12, 2016; accepted January 25, 2016. Date of publication May 9, 2016; date of current version July 7, 2016. This work was supported in parts by a Grant-in-Aid for Scientific Research (A) 26249108 and (S) 26220602 from the Japan Society for the Promotion of Science and by the JSPS Core-to-Core Program. The review of this paper was arranged by Associate Editor T. S. Wong.

H. Watanabe is with the Correlated Electronics Group, Electronics and Photonics Research Institute, National Institute of Advanced Industrial Science and Technology, Higashi, Tsukuba, Ibaraki 305-8565, Japan (e-mail: hideyuki-watanabe@aist.go.jp).

H. Umezawa is with the Advanced Power Electronics Research Center, National Institute of Advanced Industrial Science and Technology, Ikeda, Osaka 563-8577, Japan (e-mail: hitoshi.umezawa@aist.go.jp).

T. Ishikawa was with the School of Fundamental Science and Technology, Keio University, Yokohama, Kanagawa 223-8522, Japan. He is now with the Research Center for Advanced Science and Technology, The University of Tokyo, Meguro-ku, Tokyo 153-8904, Japan (e-mail: toyofumi@qc.rcast.u-tokyo.ac.jp).

K. Kaneko was with the School of Fundamental Science and Technology, Keio University, Yokohama, Kanagawa 223-8522, Japan. He is now with the Department of Precision Engineering, School of Engineering, the University of Tokyo, Bunkyo-ku, Tokyo 113-8656, Japan (e-mail: kaneko@susdesign.t.u-tokyo.ac.jp).

S. Shikata is with the Deparatment of Nanotechnology for Sustainable Energy, School of Science and Technology, Kwansei Gakuin University, Sanda, Hyogo 669-1337, Japan (e-mail: SShikata@kwansei.ac.jp).

J. Ishi-Hayase and K. M. Itoh are with the School of Fundamental Science and Technology, Keio University, Yokohama, Kanagawa 223-8522, Japan (e-mail: hayase@appi.keio.ac.jp; kitoh@appi.keio.ac.jp).

Color versions of one or more of the figures in this paper are available online at http://ieeexplore.ieee.org.

Digital Object Identifier 10.1109/TNANO.2016.2528678

I. Introduction

A SINGLE electron spin trapped by defects in diamond can function as a stable resource for a magnetic field sensor that breaks the conventional limit in spatial resolution and sensitivity at room temperature [1]–[6]. Currently, there is great interest in an emerging new field called "quantum sensing" based on the control and manipulation of single electron spins [7]. The single electron spin can be associated with a nitrogen-vacancy (NV) center known as a point defect in diamond [8], [9]. Negatively charged nitrogen-vacancy (NV^-) centers are fluorescent, and exhibit an emissive spectrum with a zero-phonon line at 638 nm [10]. The spin state of the single electron can be detected using optical pumping and photon detection of the optical transition of the NV^- centers. The primary reason for the attention devoted to diamond is that the lifetimes of the electron spin states at room temperature are much longer than those of other materials ($\sim$ milliseconds) [11], [12]. The lifetime is one of the parameters which determines the sensitivity of a device used to measure a minimally detectable magnetic field. One of the challenges here, however, is how to form NV^- optical centers and place them effectively and accurately near the surface of a diamond crystal, [13]–[18] while maintaining the long electron spin lifetime needed to produce a "quantum sensing" device. One way to achieve this is to increase the spatial resolution.

Currently, the most commonly used techniques to generate NV optical centers are ion implantation and subsequent annealing, or electron irradiation and subsequent annealing in diamond. Both are processes which produce vacancies, but which cause radiation damage upon recovering the crystal. On the other hand, herein is proposed a technique where, upon growing high quality diamond via microwave plasma-assisted chemical vapor deposition (CVD), the formation of NV centers occurs at the same time [12], [19]. We recently reported that, using optimized growth conditions, the formation of near-surface NV^- centers with 5 nm spatial resolution is possible with microwave plasma-assisted CVD, using an isotopically-enriched methane ($^{12}CH_4$), hydrogen (H_2) and nitrogen (N_2) gas mixture, delivered via a mass-flow controller during growth [20]. However, diamond growth is performed upon the entire substrate in the CVD method. This makes it difficult to use techniques associated with the adjustment of area size or position on a two-dimensional plane, such as the ion implantation technique.

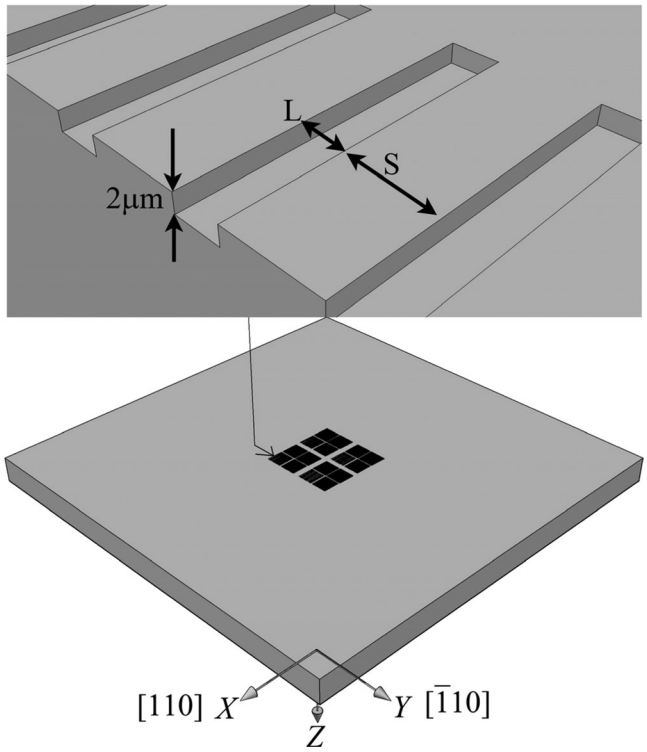

Fig. 1. Schematic of the patterned diamond substrate.

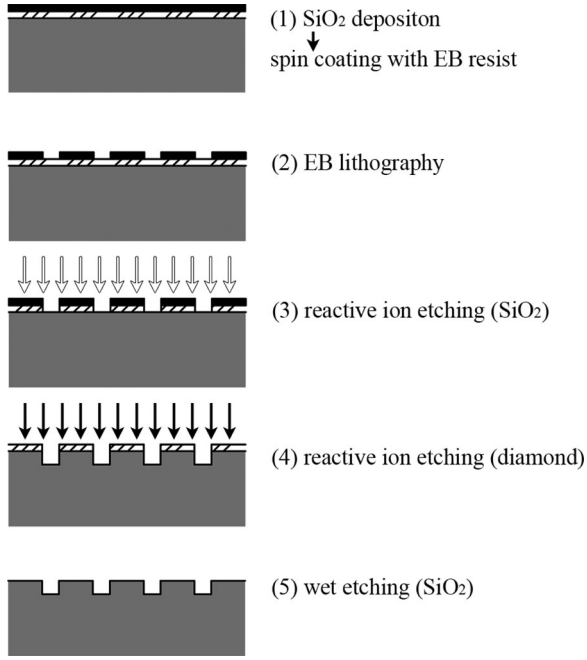

Fig. 2. Cross-section schematic of the fabrication steps for production of periodic rectangular groove lines.

Herein is proposed an approach to control not only the depth, but also the size (area) and position (in the horizontal direction), of NV^- centers by employing a CVD method only. The intensity/distribution of NV^- optical centers as observed by means of a confocal microscope photoluminescence (PL) mapping of the nitrogen-doped homoepitaxial CVD diamond indicated high contrast specific to the positions of mechanical polishing scratches on the substrate. Inspired by this result, grooves were cut into the substrate surface to form artificial polishing marks/scratches, and subsequent experiments showed that NV^- optical centers can be selectively placed inside those grooves.

II. Experimental Details

In this study, rectangular grooves were processed into the substrate using the same device fabrication techniques as are employed in the production of diamond Schottky barrier diodes [21]. Rectangular grooves 200 μm long and 2 μm deep were etched into the diamond along the [110] axis. The goal of the process was the rectangular groove structure shown in Fig. 1. By changing the groove line width (L) and spacing (S), four types of periodic artificial polishing marks or scratches were fabricated on a single substrate by lithography and dry etching processes.

Fig. 2 shows the fabrication steps employed in the generation of the periodic grooves. The substrates were synthetic type IIa (0 0 1) single-crystal diamond plates with a misorientation angle of about 0.6° as detected by X-ray diffraction. The substrate was mechanically prepolished using the scaife process to obtain a high grade surface, and then chemically cleaned. In the first fabrication step (Fig. 2, Step 1), a thin silicon dioxide (SiO_2) film was deposited via CVD using tetraethyl orthosilicate (TEOS) at 350 ºC. The film thickness was 100 nm. It was then spin-coated with an electron beam (EB) resist (ZEP520A). Then (2), EB lithography was utilized to pattern the lines/spaces on the film. In this study, four L/S patterns were produced in the EB resist: A (5/10 μm), B (2.5/5 μm), C (1/2 μm) and D (0.5/1 μm). Then (3), the SiO_2 film was etched with inductive coupled plasma (ICP) using the EB resist as a mask. The EB resist etching was carried out using tetrafluoromethane (CF_4) plasma. After removing the EB resist, the diamond was etched 2 μm deep with ICP using SiO_2 as a mask (4). A mixture of oxygen (97 sccm) and CF_4 (3 sccm) gas was used to realize a high selective ratio $>$100 and low etching damages. Finally (5), the diamond was cleaned with hydrofluoric acid (HF) and a hot acid mixture to remove the SiO_2 mask and graphitic layer.

Prior to loading into the growth chamber, the substrate was cleaned by boiling in a sulfuric acid-hydrogen peroxide mixture (SPM)-based solution, ultrasonicated in deionized water and alcohol-based solutions, etched in an HF solution, treated with RCA SC-1 (NH_4OH:H_2O_2:H_2O = 1:1:5), and finally, rinsed with deionized water. The substrate was also treated with H_2 plasma in the processing chamber for 10 min. using high purity H_2 gas ($>$9N). Diamond films were prepared from an isotopically-enriched ($>$ 99.9% for ^{12}C) $^{12}CH_4$, H_2 and N_2 mixed gas system in a microwave plasma-assisted CVD reactor, contained in a stainless-steel vacuum chamber. The feed gases were delivered via a computer-controlled mass-flow controller, and were premixed in the manifold before being injected into the growth chamber. The reaction gas was composed of 0.5% $^{12}CH_4$ in H_2. N-doping was achieved during growth by using N in the

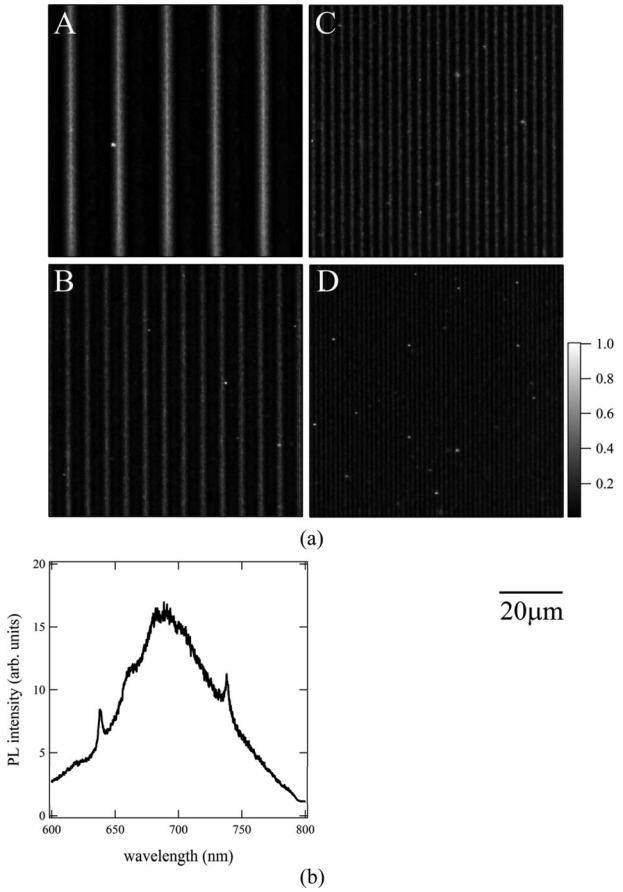

Fig. 3. (a) Confocal microscope PL images of CVD diamond layer homoepitaxialy grown. Four 80 × 80 μm areas with different groove patterns: A: L/S = 5/10 μm, B: L/S = 2.5/5 μm, C: L/S = 1/2 μm and D: L/S = 0.5/1 μm. (b) A sample PL spectrum obtained from the bright area of a PL image.

reactant gas (nitrogen to carbon ratio (N/C) = 0.0175). The total gas pressure, total gas flow rate, and input microwave power were maintained constant at 25 Torr, 400 sccm, and 750 W, respectively. The substrate temperature was 800 °C, controlled independently of the input microwave power. The deposition time was 6 h. Based on typical growth rates, the film thickness was estimated to be about 500 nm.

The optical properties of the homoepitaxial diamond thin film regions in the area of the grooves were investigated with a home-built scanning confocal microscope at room temperature. PL was excited with a continuous-wave 532 nm laser. The laser light was focused onto the sample by an objective lens with 100× magnification and a numerical aperture of 0.9. The PL signal was detected either with a charge coupled device spectrometer for spectra, or via an avalanche photodiode detector (APD) for images. An optical band pass filter, with transmission from 600 nm to 800 nm, was placed in front of the APD for wavelength selection.

III. Results and Discussion

Fig. 3(a) shows the PL images obtained using the confocal microscope system for each of the four types of patterns. The observation area is 80 μm × 80 μm, and the resolution is 0.2 μm. The PL signal was not uniform over the area, but showed a cyclic pattern along the y-axis. This cyclic pattern matches the pattern of the grooves. The contrast ratio of bright areas (maximum average PL signal of bright areas = I_{bright}) to dark areas (minimum average PL signal of dark areas = I_{dark}) obtained from patterns A, B, C and D decreased as the line width and spacing decreased ($I_{\mathrm{bright}}/I_{\mathrm{dark}} \approx 73, 12, 7,$ and 4, respectively).

Fig. 3(b) shows, as an example, the PL spectrum (600–800 nm) obtained from a bright area of pattern A. In the spectrum, the zero-phonon line at 638 nm due to the NV^- centers and their phonon replicas can be clearly identified. In addition, this spectrum contains a single, narrow peak at 738 nm. The peak position of the maximum was found by fitting a Gaussian distribution to the data. This 738 nm peak is very close to the emission of a self-interstitial defect (1.685 eV center) at 736 nm, [22] a silicon vacancy complex (Si center) at 737.1 nm, [23] or a neutral single vacancy (GR1 center) at 741 nm [24]. The peak tends to be subject to the groove processing conditions (groove line width and processing method), and moreover, no signal indicating Si atoms was detected via secondary ion mass spectrometry (SIMS) in the groove region of the sample. Therefore, at present, the 738 nm emission is believed to be related to presence of self-interstitial defects, neutral single vacancies, or other possible defect complexes. At minimum, these results indicate that the NV^- centers, which are related to the PL intensity in the visible range, are distributed spatially within the grooves.

In the epitaxial growth of thin films, surface morphologies reflecting the growth history provide hints to understanding the mechanism of growth. Fig. 4(a) shows a circularly polarized light-differential interference contrast optical microscopy image of the surface after epitaxial growth of the four types of patterns. As seen here, the normal epitaxial surface area, E, is characterized by a macro zigzag pattern. This surface morphology is typical of a step flow growth process, and is expected for the azimuthal miscut angle of this substrate, as proposed by Lee *et al.* [25] for homoepitaxial CVD diamond growth on (0 0 1) planes. In fact, the azimuthal miscut angle (ϕ) of the substrate used in this work is tilted about 49° from the [1 1 0] direction toward the [1 0 0] direction. Meanwhile, all four of the grooved areas demonstrate growth in which the zigzag morphology is suppressed, the flatness is improved, and the macro steps are oriented parallel to the grooves (along the [1 1 0] direction). So, in the homoepitaxial diamond growth on this diamond (0 0 1) surface, the growth occurs through a lateral movement or step flow of the preexisting step edges along the ⟨1 1 0⟩ directions. Thus, for example, if the substrate were miscut parallel to $[\bar{1}\ 1\ 0]$ (that is, step edges along the [1 1 0] direction), the macro steps would not be zigzag they would exhibit a straight pattern. Therefore, inhibition of the zigzag pattern observed in the area of the grooves can be understood to be due to the fact that processing of the rectangular grooves causes a significant change in the miscut angle at groove locations on the substrate surface.

Fig. 4(b) shows a cross-section SIMS image of the ^{13}C concentration for a diamond thin film grown on a 5 μm groove line-patterned diamond substrate (pattern A). (Lower ^{13}C concentration is displayed darker.) The ion image of the *YZ* axis is

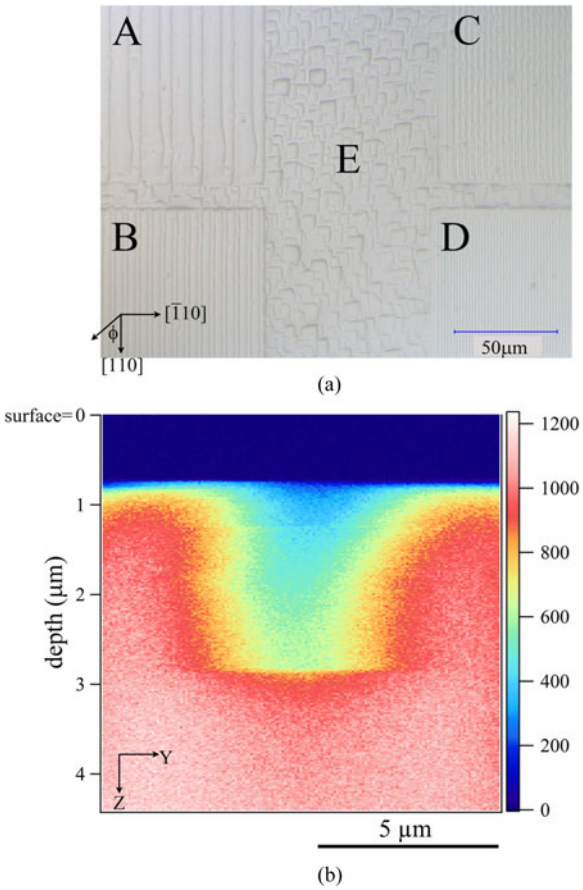

Fig. 4. (a) C-DIC optical microscope image of the surface after homoepitaxial CVD diamond thin film growth on areas with grooves (A–D) and on the normal epitaxial surface without grooves (E). (b) Cross-section SIMS ion image of ^{13}C concentration for the CVD diamond layer homoepitaxialy grown on a 5 μm groove line-patterned diamond substrate.

constructed from 270 ion image basic data, each with a sputter depth of 16 nm. It is clearly seen that the 2 μm deep grooves have been completely covered by the diamond. Based on the vertical thickness and growth time, the growth rate of the normal epitaxial surface area is expected to be about 0.4 μm/h. On the other hand, it should be noted that from Fig. 4(b), the growth rate at a groove with a (0 0 1) bottom is about 1.6 μm/h, four times higher than that at the (0 0 1) normal epitaxial surface. The velocity of growth of the crystal face in step flow growth mode is sensitive to the density of the steps, which in turn depends on the value of the misorientation angle [25]. One possible reason for this is that the larger growth rate in the groove occurs because of the presence of higher step density caused by the tilt angles of the etched vertical side walls or corners. This suggestion may be supported by the cross-section SIMS image in Fig. 4(b) where the side walls are clearly slightly tilted. On the other hand, another possible reason for the relatively larger growth velocity is a change in the growth conditions caused by the local surface structure; that is, the grooves. Of note, the growth parameter, [26]–[28] which describes the ratio of relative growth rates on the $\{0\,0\,1\}$, $\{1\,1\,0\}$, $\{1\,1\,1\}$ and $\{1\,1\,3\}$ planes, is sensitive to growth conditions. In this case, because the $\{0\,0\,1\}$ planes have the lowest growth rate [29], the filling process of the rectangular grooves may result from selective epitaxial growth under another index surface such as $\{1\,1\,1\}$ or $\{1\,1\,3\}$ [30]. Although further research is required to investigate this growth mechanism, these features suggest that at least the corners and the etched vertical side walls of the rectangular grooves play a major role in the filling process of rectangular grooves.

In typical CVD diamond growth, there are some common (limiting) characteristics, such as that impurities begin to be incorporated when the growth rate exceeds the critical growth rate, [31], [32] and that the amount of impurities incorporated is proportional to the growth rate [33]. These experiments clearly show that, by creating fine grooves on a substrate surface, the growth rate can be increased locally, and simultaneously, vacancies (as well as the nitrogen required for NV center formation) can be supplied.

IV. Conclusion

In conclusion, this is an approach, employing a microwave plasma-assisted CVD method only, that has the ability to control not only the depth of NV^- optical centers formed inside an isotopically-controlled diamond thin film, but also their size (area) and position in the horizontal direction. We have found that, by generating the proper pattern of fine grooves on the substrate surface, the growth rate can be increased locally, and at the same time, nitrogen and the vacancies required for NV^- center formation can be supplied. These findings suggest that producing groove patterns on a surface might provide an effective technique for forming NV^- optical centers of a desired size at a desired position near the surface. This process can be accomplished without reduction of device performance, which is limited by traditional ion implantation or EB-induced defects. In addition to the selectable size and density of the NV^- optical centers, the orientation of these centers plays an important role in the production of high sensitivity diamond quantum sensors and has been difficult to control with conventional techniques. Approaches for orientation control will likely also be available using this CVD method.

Acknowledgment

The authors would like to thank Mr. S. Tomizawa, Mr. K. Ohashi, and Mr. T. Gomi at Keio University for PL measurements. The authors would also like to thank Dr. Y. Kato at National Institute of Advanced Industrial Science and Technology for X-ray diffraction measurements.

References

[1] M. L. Markham *et al.*, "CVD diamond for spintronics," *Diamond Related Mater.*, vol. 20, pp. 134–139, 2011.
[2] R. Schirhagl, K. Chang, M. Loretz, and C. L. Degen, "Nitrogen-vacancy centers in diamond: nanoscale sensors for physics and biology," *Annu. Rev. Phys. Chem.*, vol. 65, pp. 83–105, 2014.
[3] S. Prawer and I. Aharonovich, Eds., *Quantum Information Processing With Diamond: Principles and Applications (Series in electronic and Optical Materials, no. 63)*, Amsterdam, The Netherlands: Elsevier, 2014.
[4] M. Loretz, T. Rosskoph, and C. L. Degen, "Radio-frequency magnetometry using a single electron spin," *Phys. Rev. Lett.*, vol. 110, pp. 017602-1–017602-5, 2013.

[5] V. S. Perunicic, L. T. Hall, D. A. Simpson, C. D. Hill, and L. C. L. Hollenberg, "Towards single-molecule NMR detection and spectroscopy using single spins in diamond," *Phys. Rev. B*, vol. 89, pp. 054432-1–054432-7, 2014.
[6] L. Rondin *et al.*, "Magnetometry with nitrogen-vacancy defects in diamond," *Rep. Progress Phys.*, vol. 77, pp. 056503-1–056503-26, 2014.
[7] K. M. Itoh and H. Watanabe, "Isotope engineering of silicon and diamond for quantum computing and sensing applications," *MRS Commun.*, vol. 4, pp. 143–157, 2014.
[8] M. W. Doherty *et al.*, "The nitrogen-vacancy colour centre in diamond," *Phys. Rep.*, vol. 528, pp. 1–45, 2013.
[9] F. Jelezko and J. Wrachtrup, "Single defect centres in diamond: A review," *Phys. Status Solidi (a)*, vol. 203, no. 13, pp. 3207–3225, 2006.
[10] A. M. Zaitsev, *Optical Properties of Diamond: A Data Handbook*. New York, NY, USA: Springer, 2001.
[11] G. Balasubramanian *et al.*, "Ultralong spin coherence time in isotopically engineered diamond," *Nature Mater.*, vol. 8, pp. 383–387, 2009.
[12] T. Ishikawa *et al.*, "Optical and spin coherence properties of nitrogen-vacancy centers placed in a 100 nm thick isotopically purified diamond layer," *Nano Lett.*, vol. 12, pp. 2083–2087, 2012.
[13] M. Loretz, S. Pezzagna, J. Meijer, and C. L. Degen, "Nanoscale nuclear magnetic resonance with a 1.9-nm-deep nitrogen-vacancy sensor," *Appl. Phys. Lett.*, vol. 104, pp. 033102-1–033102-5, 2014.
[14] B. K. Ofori-Okai *et al.*, "Spin properties of very shallow nitrogen vacancy defects in diamond," *Phys. Rev. B*, vol. 86, pp. 081406-1–081406-5, 2012.
[15] K. Ohno *et al.*, "Engineering shallow spins in diamond with nitrogen delta-doping," *Appl. Phys. Lett.*, vol. 101, pp. 082413-1–082413-5, 2012.
[16] T. Staudacher *et al.*, "Nuclear magnetic resonance spectroscopy on a (5-nanometer)^3 sample volume," *Science*, vol. 339, pp. 561–563, 2013.
[17] H. J. Mamin *et al.*, "Nanoscale nuclear magnetic resonance with a nitrogen-vacancy spin sensor," *Science*, vol. 339, pp. 557–560, 2013.
[18] J. Wrachtrup, F. Jelezko, B. Grotz and L. McGuinness, "Nitrogen-vacancy centers close to surfaces," *MRS Bull.*, vol. 38, pp. 149–154, 2013.
[19] M. Lesik *et al.*, "Preferential orientation of NV defects in CVD diamond films grown on (113)-oriented substrates," *Diamond Related Mater.*, vol. 56, pp. 47–53, 2015.
[20] K. Ohashi *et al.*, "Negatively charged nitrogen-vacancy centers in a 5 nm thin ^{12}C diamond film," *Nano lett.*, vol. 13, pp. 4733–4738, 2013.
[21] H. Umezawa, M. Nagase, Y. Kato, and S. Shikata, "High temperature application of diamond power device," *Diamond Related Mater.*, vol. 24, pp. 201–205, 2012.
[22] A. Mainwood, "Modelling of interstitial-related defects in diamond," *Diamond Related Mater.*, vol. 8, pp. 1560–1564, 1999.
[23] C. D. Clark, H. Kanda, I. Kiflawi, and G. Sittas, "Silicon defects in diamond," *Phys. Rev. B.*, vol. 51, pp. 16681–16688, 1995.
[24] G. Davies, S. C. Lawson, A. T. Collins, A. Mainwood, and S. J. Sharp, "Vacancy-related centers in diamond," *Phys. Rev. B*, vol. 46, pp. 13157–13170, 1992.
[25] N. Lee and A. Badzian, "A study on surface morphologies of (001) homoepitaxial diamond films," *Diamond Related Mater*., vol. 6, pp. 130–145, 1997.
[26] C. Wild *et al.*, "Chemical vapour deposition and characterization of smooth {100}-faceted diamond films," *Diamond Related Mater.*, vol. 2, pp. 158–168, 1993.
[27] F. Silva *et al.*, "High quality, large surface area, homoepitaxial MPACVD diamond growth," *Diamond Related Mater.*, vol. 18, pp. 683–697, 2009.
[28] A. Bogatskiy and J. E. Butler, "A geometric model of growth for cubic crystals: Diamond," *Diamond Related Mater.*, vol. 53, pp. 58–65, 2015.
[29] R. E. Clausing, "Diamond morphology," in *Handbook of Industrial Diamonds and Diamond Films*, M. A. Prelas, G. Popovici, and L. K. Bigelow, Eds., New York, NY, USA: Marcel Dekker, 1998, ch. 2, pp. 19–47.
[30] H. Kato *et al.*, "Selective growth of buried n^+ diamond on (001) phosphorus-doped n-type diamond film," *Appl. Phys. Express*, vol. 2, pp. 055502-1–055502-3, 2009.
[31] H. Okushi, "High quality homoepitaxial CVD diamond for electronic devices," *Diamond Related Mater.*, vol. 10, pp. 281–288, 2001.
[32] H. Watanabe, S. G. Ri, S. Yamanaka, D. Takeuchi, and H. Okushi, "High-quality homoepitaxial diamond film growth," *New Diamond Frontier Carbon Technol.*, vol. 12, no. 6, pp. 369–379, 2002.
[33] M. Ogura, H. Kato, T. Makino, H. Okushi, and S. Yamasaki, "Misorientation-angle dependence of boron incorporation into (001)-oriented chemical-vapor-deposited (CVD) diamond," *J. Cryst. Growth*, vol. 317, pp. 60–63, 2011.

Authors' photographs and biographies not available at the time of publication.